



Contents lists available at ScienceDirect

# Engineering Failure Analysis

journal homepage: [www.elsevier.com/locate/engfailanal](http://www.elsevier.com/locate/engfailanal)

## Shark attacks on offshore streamer cables

Terje Rølvåg\*, Axel B. Hagen, Tarald B. Hagen

NTNU, Faculty of Engineering Science and Technology, 7491 Trondheim, Norway



### ARTICLE INFO

#### Keywords:

Shark attacks  
Marine seismic  
Streamer cables  
FEA

### ABSTRACT

In the search for new subsea oil fields, geologists use vessels to tow streamer cables, which collect seismic data. This activity attracts bull sharks to the magnetic streamer fields causing shark attacks and hence losses and delays. This paper discusses how shark attacks on streamer cables can be modelled and simulated in cable design and optimization processes. In order to generate a representative simulation model, a large and authentic bull shark jaw was 3D-scanned. The shark jaw was converted to a CAD-model utilizing reverse engineering applications. Numerical models of the streamer cables, capturing the response with respect to friction properties and failure criteria's, were benchmarked using quasi-static compression tests. Additionally, dynamic bite and impact simulations replicating the shark attack on streamer cables have been conducted. The physical compression tests and simulations show that the streamer cable FE-models are valid. The results indicate that a shark bite can be sufficient to critically damage the cable, but the bite resilience of the streamer cable is strongly correlated to the shark speed upon impact.

### 1. Introduction

In marine seismic surveys, purpose-built vessels tow a number of cables called streamers. The streamer cables are equipped with hydrophones that receive the returned signals initiated from a seismic source, typically a series of air guns towed behind the ships stern [1]. A line of streamers is deployed at 5–20 m depth, and each streamer is typically 8 km long. Marine seismic surveys generate a vast quantity of sub-surface information. The data form the basis for the capture of important geological information from the sub-surface images derived from the acoustic wave reflection.

In specific areas, equipment loss due to shark attacks on streamer cables is a serious problem in terms of time delays and economic loss for the operator [2]. One related research question is how virtual shark attacks on streamer cables can be modelled and simulated to support cable design and optimization. This paper presents how the authors have performed virtual shark attacks in Abaqus to analyze the streamer cable's resilience against shark attacks. The streamer cable models are verified by physical quasi-static compression tests. Models, load cases, methods and simulation results are presented.

### 2. The bull shark (load case)

The bull shark, is a cartilaginous fish, meaning the skeleton consists exclusively of cartilage. The bull shark's average body mass and length are 130 kg and 2.4 m, respectively. It usually thrives in tropical to subtropical coastal waters [1], areas where oil

\* Corresponding author at: Department of Mechanical and Industrial Engineering, Norwegian University of Science and Technology (NTNU), Richard Birkelands vei 2b, 7491 Trondheim, Norway.

E-mail addresses: [terje.rolvag@ntnu.no](mailto:terje.rolvag@ntnu.no) (T. Rølvåg), [axel.hagen@outlook.com](mailto:axel.hagen@outlook.com) (A.B. Hagen), [tarald.hagen@outlook.com](mailto:tarald.hagen@outlook.com) (T.B. Hagen).

<https://doi.org/10.1016/j.engfailanal.2020.104403>

Received 14 August 2019; Received in revised form 16 December 2019; Accepted 14 January 2020

Available online 21 January 2020

1350-6307/ © 2020 Elsevier Ltd. All rights reserved.

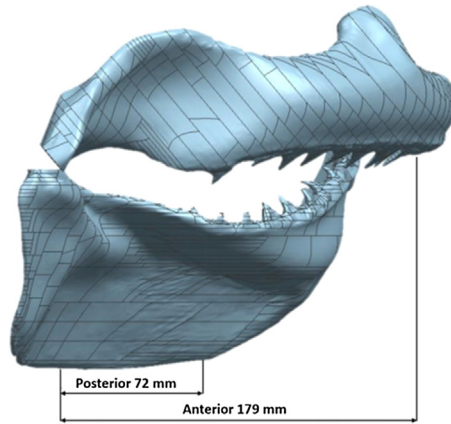


Fig. 1. Bull shark jaw model.

companies have encountered problems with sharks attacking the streamer cables [2,3].

According to Huber et al. [4], head width is the best indicator of bite force. Our scanned bull shark jaw has a width of 40 cm, corresponding to an anterior bite force of 1580 N. A simple static equilibrium model shown in Fig. 1 suggests that the acquired bull shark was able to generate a torque of 282 Nm about the jaw joint.

The bite kinematics is a vital factor when simulating the dynamics of a shark attack. To date, no research validates the bite velocity of a bull shark [14], but based on studies of other sharks shown in Table 1, the bite time of a typical bull shark is estimated.

According to Table 1, the clamping time of the jaws are relatively independent of both shark species and size. Due to the resemblances between a white shark and a bull shark, it is reasonable to assume that the described bite mechanism in Fig. 2 also applies to bull sharks [4–7]. The illustration suggests that the biting mechanism of a shark is not a “straightforward” clamping movement. Because the mandible of cartilaginous fishes are not attached to the cranium, the jaw is allowed independent movement relative to the cranium. Upon biting, the mandible (lower jaws) move backward and downward, while the maxilla (upper jaw) move upward (B). Upon clamping the upper jaw rotates forward and downward, exposing the upper teeth (C). Snout drop causes retraction of the jaws to its normal position (D). Sharks (also bull sharks) are known to utilize lateral head shaking to cut through the prey [6].

Based on these assumptions, only the clamping sequence is considered in the bite simulations and the average clamping time is set to 200 [ms]. The shark’s simulated impact speed was set to the worst-case scenario of 19 km/h. According to [3], bull sharks can achieve a swim speed of 19 km/h upon pray capture, while the average cruising speed is 8 km/h.

### 3. Methods

The goal was to create a realistic simulation approach to a shark attack on a streamer cable. A quasi-static simulation was used to verify the cable response to transverse compression. The quasi-static simulation was set up to replicate the physical test, and the virtual models were tuned according to the test results. Additionally, dynamic simulations replicating the shark attack on streamer cables has been conducted.

Abaqus/Explicit was selected since a nonlinear response due to complex contact definitions and excessive high-speed deformations was expected [13]. General contact was used to enable simple contact definition between the complex shark jaw and cable stress members. Energy outputs were used to verify the Abaqus models and simulations.

The following criteria were used to validate the quasi-static simulations:

- The kinetic energy (ALLKE) must not be affected by the applied mass scaling
- Artificial strain energy (ALLAE) must be less than 10% of the internal energy (ALLIE).
- Total energy (ETOTAL) must be constant.

The following criteria were used to validate the dynamic bite and impact simulations:

Table 1

Comparison of bite kinematic between sharks.

	Six gill [8]	Great White [5,9,15]	Dogfish [8,10]	Lemon [11]	Nurse [12]
Method of capture	Ram/suck	Bite and ram	Ram/suck	Ram	Suction
Shark size	2–3.5	3.5	0.5–0.7	0.7–0.8	0.6–1.0
Total bite time [ms]	547	443	302	309	100
Clamping time [ms]	196	202	192	218	–

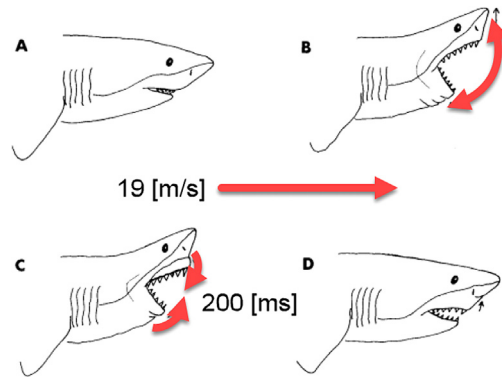


Fig. 2. Bite pattern of a great white shark.

- Artificial damping energies such (ALLVD), artificial strain energy (ALLAE) and mass scaling work (ALLWM) must be negligible compared to (ALLKE).
- Total energy (ETOTAL) should be constant.

#### 4. Cable model

The most critical parts of a streamer cable are skin, gel, spacer, and stress-members [2]:

- **Skin:** The skin protects the inside elements, transfers acoustics and control the buoyancy. The skin material is unreinforced Termoplastics
- **Gel:** The gel fills open voids in the cable and is pressurized in order to expand the plastic skin. It works as an insulator and is used as an instrument to create neutral buoyancy. The gel filler is not modelled.
- **Spacer:** The spacer keeps everything in place, and avoids excessive load on electrical components. The spacers are positioned regularly during the length of the cable. The spacer material is polyamide Zytel (7300 T series).
- **Stress-members:** The stress-members are made of Kevlar and handle high tensile load which occurs during operation. A jacket protects the Kevlar. It also keeps the Kevlar in position and works as an UV protector (see Fig. 3).

The streamer cable model was created in NX. The models were simplified and only load carrying internal components were explicitly modelled (spacer, skin and stress members). The dimensions are given in Table 2:

Bilinear material models were assigned and tuned for the different parts. Strain-based damage definition was utilized, and the fracture strain adjusted in accordance with results from the physical quasi-static tests. Initially, all fracture strains were set equal to the maximum plastic strain and step wise reduced. Material data were obtained from uniaxial tensile tests. Therefore, the fracture strain is related to the distinctive load regime which the cables are exposed to in the current simulations. The post-damage behavior of the materials in the streamer cables are not considered. Hence, the damage evolution is set to zero in Abaqus, i.e., the material will break immediately after critical strain value is satisfied.

#### 5. The quasi static test on spacer

Quasi-static simulation was set up to represent the physical test as shown in Fig. 4. The purpose was to identify, model and

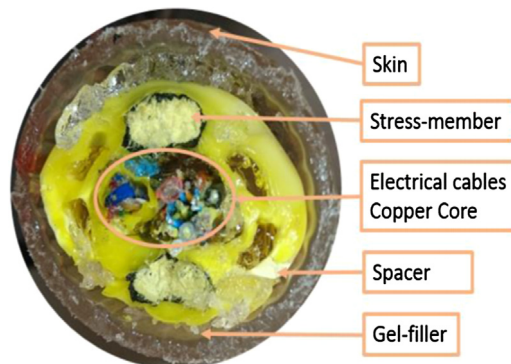


Fig. 3. The cross section adjacent to space.

**Table 2**  
The cable properties.

	Outer radius [mm]	Cross section area [mm <sup>2</sup> ]	Mass [kg/100 m]
Skin	27.5	566	65.12
Stress members	–	71.7	20.64
Spacer	24	702	12.87

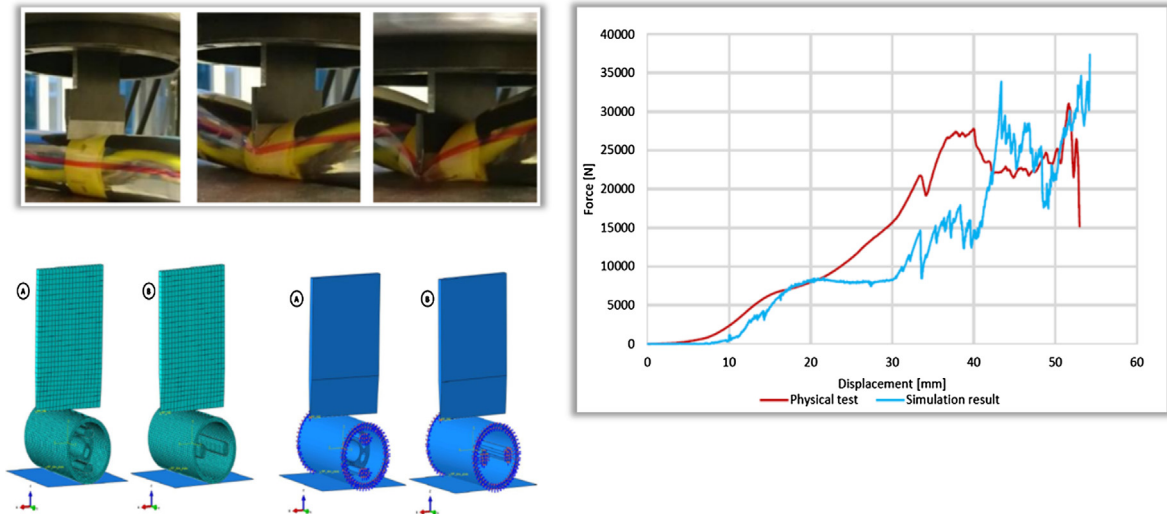


Fig. 4. Quasi-static test on spacer.

validate the physical properties of the cable cross section at the spacer. The displayed response corresponds to the tuned fracture and friction properties shown in Table 3.

A total of 7 deformation modes were observed and illustrated in Fig. 5. In mode (1), initial compression of the entire cable structure occurs, and the skin deforms plastically. The current mode generates a reaction force of 0.83 kN. Subsequently, the skin ruptures and deformation of the spacer is initiated, producing a force of 7.8 kN in mode (2). Deformation mode (3) is characterized by a constant reaction force due to the collapse of the spacer, as the middle section folds towards the skin. In mode (4) the spacer tears open, and the upper stress member undergoes shear deformation, generating several peaks as the elements in the stress member fails. The highest peak force is approximately 17 kN. The subsequent deformation mode (5) depicts shear deformation of the spacer middle section and initial failure of the second stress member, where the reaction force peaks at 34 kN. Mode (6) correlates to shear deformation of the second stress-member, the reaction force drops to 17.5 kN due to tearing. The final deformation mode (7) discloses the shear deformation of the remaining spacer and skin material, the force increases due to skin stacking towards the bottom plate culminating in a peak force of 37.4 kN.

**6. The quasi static test adjacent to spacer**

Fig. 6 shows the reaction force versus cable intrusion from the quasi-static simulations in Abaqus plotted against the results from the physical test. The displayed response corresponds to the tuned fracture and friction properties shown in Table 3.

A relatively good correlation between the force-displacement curves is observed until 40 mm penetration. Then the simulation and test results deviate due to the lack of filler materials. This is not considered important since the stress members will rupture at smaller intrusion depths in a shark attach due to the cable tension.

In the absence of the spacer, only three deformation modes are observed. The first mode is characterized by elastic compression of the cable structure and deformation of the skin. The reaction force increases slowly to approximately 0–9 kN. The first peak at 6.3 kN in mode (2), relates to skin rupture and initial penetration of the stress-members. Subsequent stress-member shear deformation

**Table 3**  
Fracture strain and friction values (true strain).

Part	Initial fracture strain [%]	Tuned fracture strain [%]	Friction
Skin	169	4	0.25
Spacer	> 100	110	0.25
Stress member	3.9	2	0.25

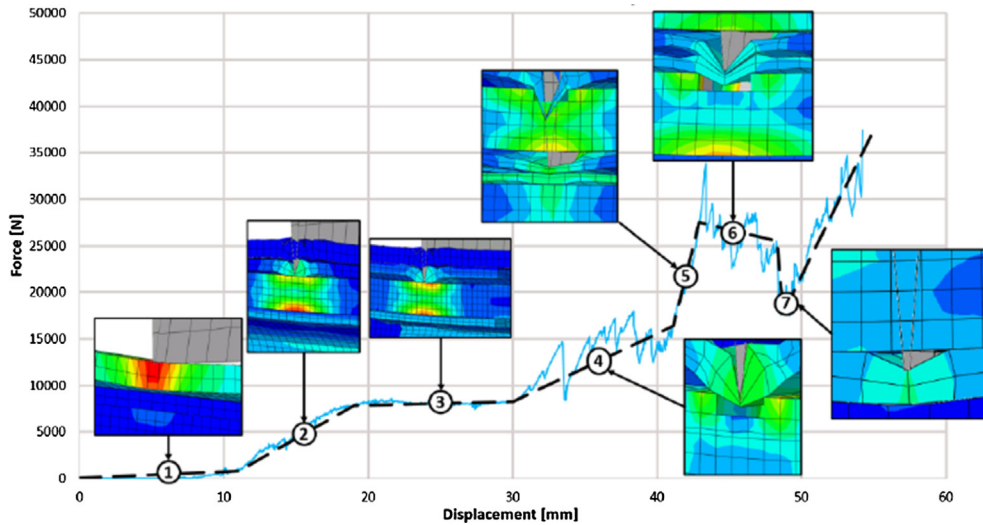


Fig. 5. Quasi-static test on spacer failure modes.

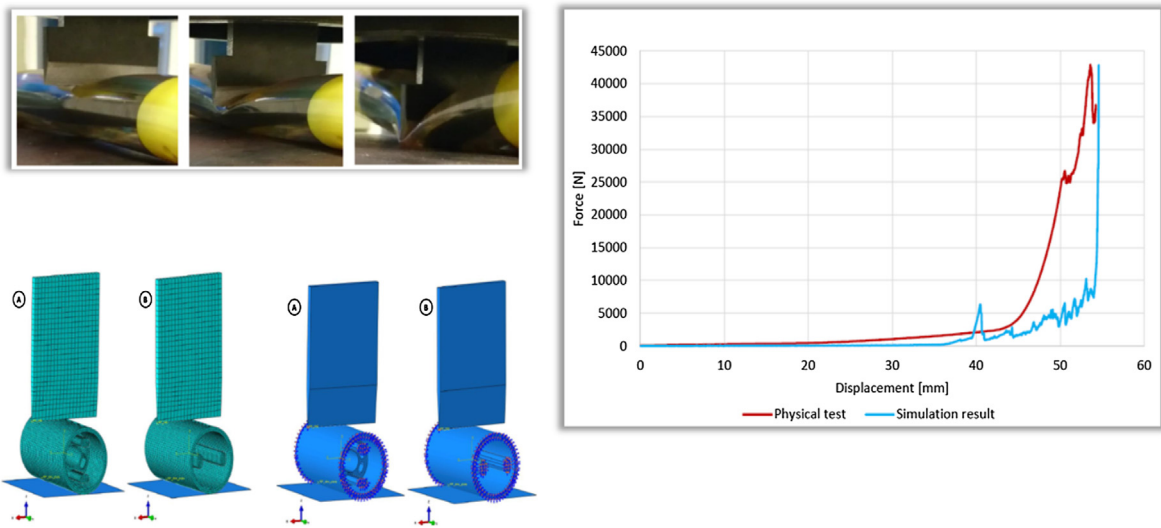


Fig. 6. Quasi-static test adjacent to spacer results.

generates a reaction force of 8.2 kN. Finally, the skin stacks against the bottom plate in deformation mode (3) (see Fig. 7).

### 7. Tuning of cable properties

Empirical tuning of the friction properties and failure criteria shown in Table 3 required numerous simulations before the correlation with the quasi-static physical tests shown in Figs. 4 and 6 were achieved. The tuning was automated by the use of a Python script in Abaqus. All simulations were initially run with a high mass scaling factor and gradually reduced until its influence on the kinetic energy was negligible compared to the strain and elastic energy levels.

### 8. The bull shark jaw model

An authentic bull shark jaw was 3D-scanned and converted to solid geometry using reverse engineering tools in NX. Geomagic Studio was used to clean the scanned geometry shown in Fig. 8. The CAD model was meshed in NX Simcenter with 4 node C3D4 tetrahedral elements with an element size of 6 mm. These elements are not fit for stress analysis but they capture the shape of head and teeth's and hence the correct impact/contact surface. In this study, the intention was not to predict shark stress or headache!

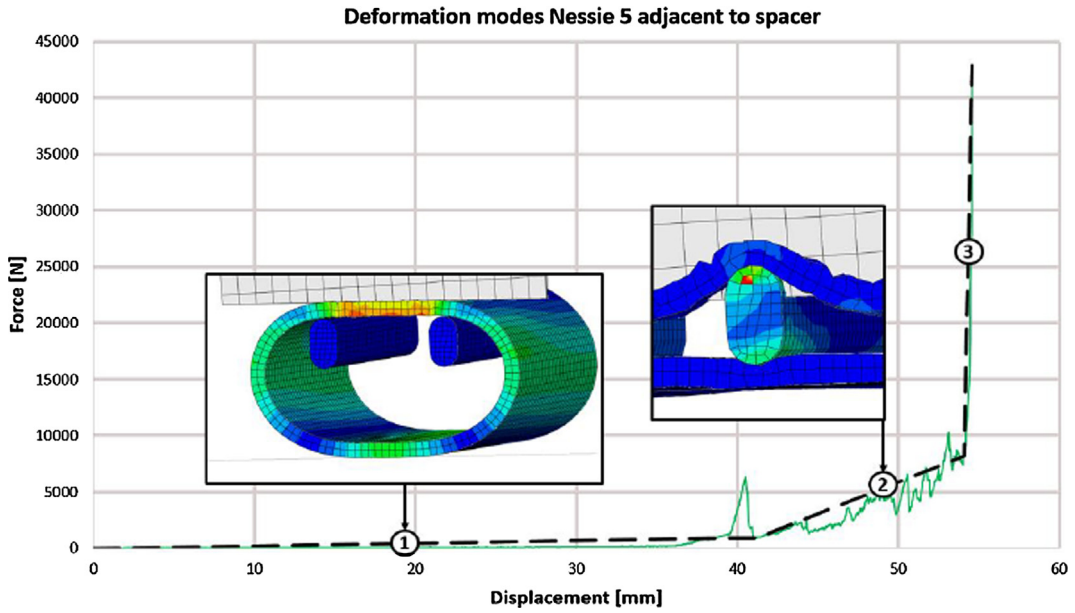


Fig. 7. Quasi-static test adjacent to spacer failure modes.

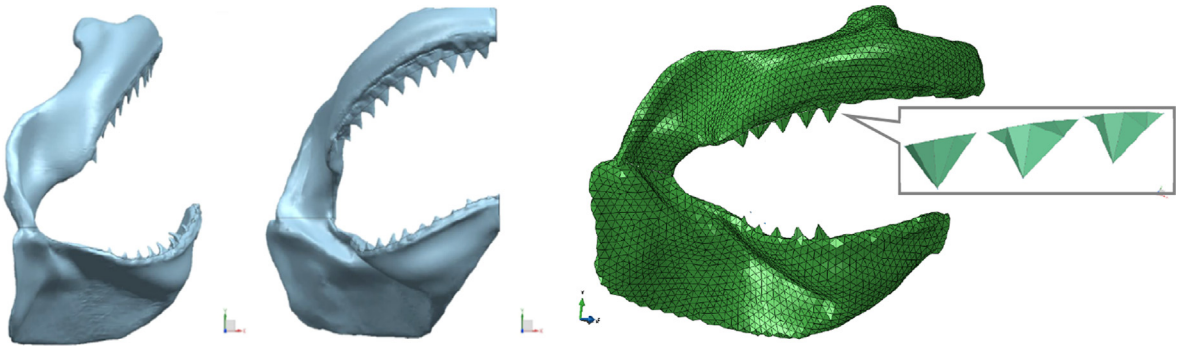


Fig. 8. Solid geometry CAD and FE model.

9. Load case 1: The shark bite simulation and results

In Section 2 the bite force was estimated to 1580 N. The bite speed is further estimated to 4.36 rad/sec based on a bite duration of 200 ms and 50°. The length from the snout to the first gill is 21.2% of the total body length, giving a head mass of approximately 34 kg [4]. The initial shark bite speed is implemented as an angular velocity field in the jaw joint as shown in Fig. 9. Consequently,

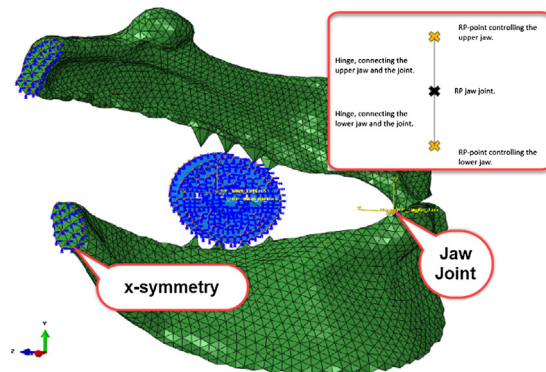


Fig. 9. Shark bite simulation setup.

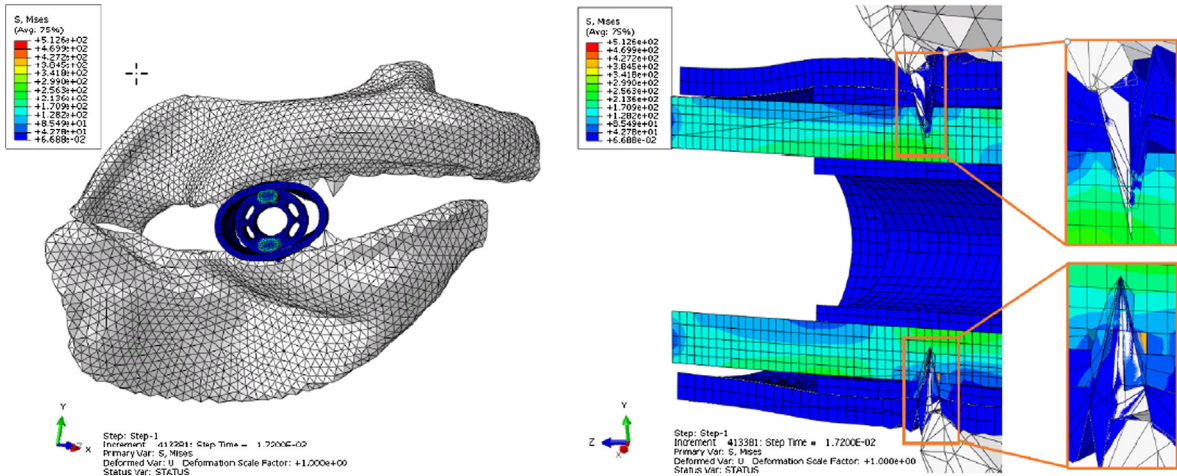


Fig. 10. Shark bite on spacer simulation results.

Abaqus calculates the actual velocity based on the inertia of the shark jaw and cable resistance during the shark bite. The cable model is constrained in the axial direction at both ends introducing axial forces during bite and impact simulations

The applied bite load on spacer is not sufficient to achieve full closure of the jaws. The teeth penetrate half way through the stress-members, causing failure of several elements but not fatal damage as shown in Fig. 10.

The shark bite load adjacent to spacer shows similar results. The bull shark is able to obtain full closure of the jaws. However, no severe damage is observed neither on the skin or the stress-members (see Fig. 11).

In regards of the streamer cables resilience towards shark bite, the results from the dynamic bite simulations indicate that the isolated shark bite mechanism alone, is not sufficient to inflict a critical damage on the streamer cables.

10. Load case 2: The shark impact simulation and results

The shark impact load on spacer is critical. Fig. 12 shows the deformation of the streamer cable when the first stress member fractures (B) and cable post rupture (A). Due to the applied stress-member tension, fracture is obtained shortly after teeth penetrates the first stress member.

The shark impact load adjacent to spacer is also critical. Fig. 13 shows the post failure deformation of the streamer cable when rammed adjacent to spacer. Similarly, for the cable on spacer analysis, the stress-members fracture upon skin and teeth penetration.

11. Summary

Based on the results from the physical quasi-static compression tests, it is reasonable to conclude that the FE-streamer cable model

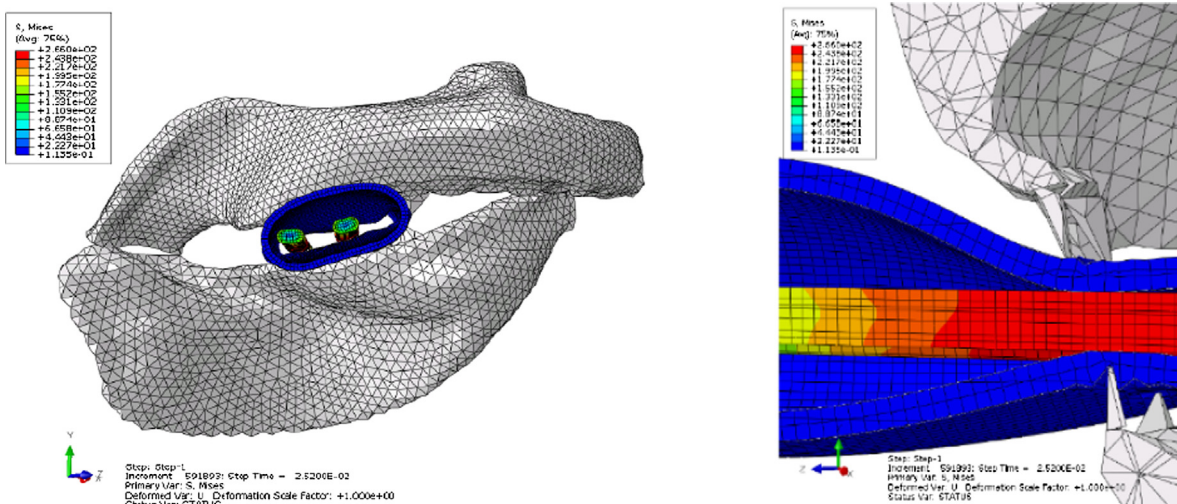


Fig. 11. Shark bite adjacent to spacer simulation results.

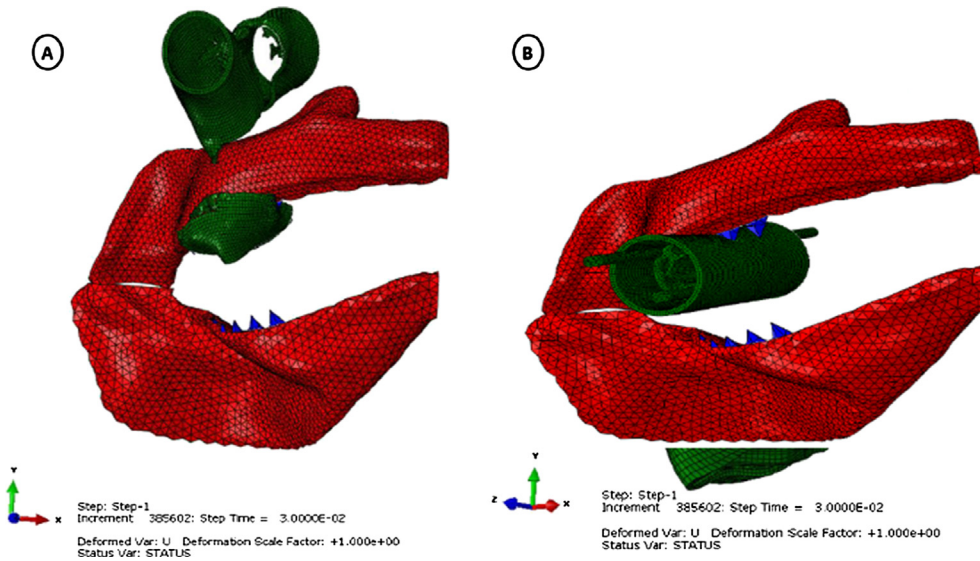


Fig. 12. Shark impact on spacer simulation results.

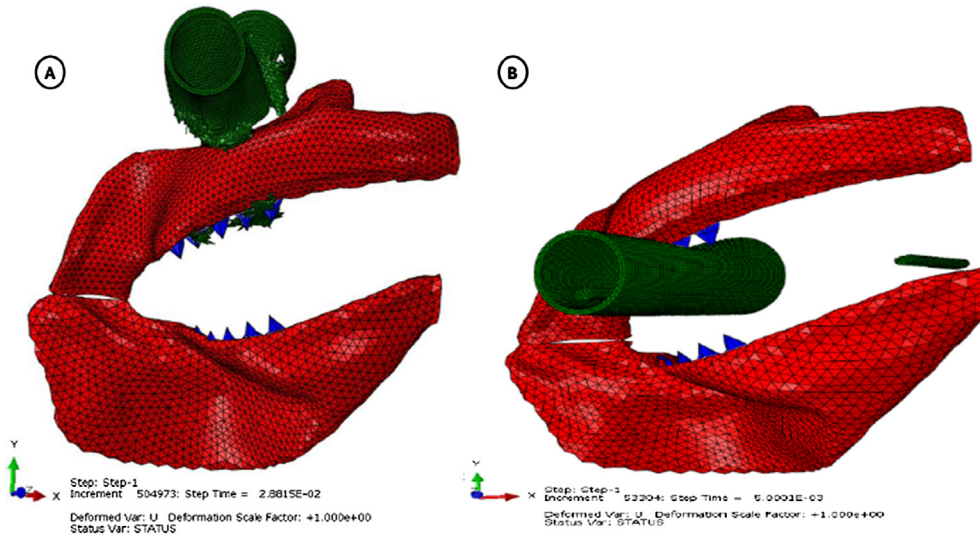


Fig. 13. Shark impact adjacent to spacer simulation results.

is applicable to future cable design and optimization. Main error sources are cable tension and gel filler effects. Considering the assumptions made, the applied failure criteria and friction properties give acceptable correlation between simulations and physical test.

The results from the dynamic bite and impact analyzes indicate that the isolated shark bite, is not sufficient to inflict a critical damage on the streamer cables. However, simulation results show that the amount of energy required to initiate stress-member failure is within close range. The authors therefore conclude that a combination of the shark bite and impact speed, is necessary to obtain a critical damage on the stress-members. The bite resilience of the streamer cable is strongly correlated to the shark speed upon impact.

These results are used in the design of a new generation streaming cables with improved shark bite resilience. Those results are currently confidential but the shark head model is available for public use.

#### Declaration of Competing Interest

The authors declared that there is no conflict of interest.

## Acknowledgements

Thanks to Svein Arne Frivik and Fabien Guizelin at WesternGeco for both technical and financial support. Thanks also to Bård Eker at Ekerdesign for an excellent shark head scan job. The corresponding author also acknowledges the contributions from his current employers SINTEF OCEAN and NTNU Dept. of Ocean Operations and Civil Engineering.

## References

- [1] R.E. Sheriff, L.P. Geldart, *Exploration Seismology*, Cambridge University Press, 1995.
- [2] Fabien Guizelin, WesternGeco, WesternGeco, 2017–2018.
- [3] SoftSchools, Bull shark facts, 2017. [http://www.softschools.com/facts/animals/bull\\_shark\\_facts/287/](http://www.softschools.com/facts/animals/bull_shark_facts/287/) (14.02.2017).
- [4] Daniel R. Huber, Julien M. Claes, Jérôme Mallefet, Anthony Herrel, Is extreme bite performance associated with extreme morphologies in sharks? *Physiol. Biochem. Zool.* 82 (1) (2009).
- [5] Timothy C. Tricas, Feeding ethology of white shark, *carcharodon carcharias*, *South. Calif. Acad. Sci., Memoirs vol. 9*, (1985).
- [6] P.J. Motta, C.D. Wilga, Advances in the study of feeding behaviors, mechanisms, and mechanics of sharks, *Environ. Biol. Fishes* 60 (1) (2001) 131–156.
- [7] James J. Powlik, On the geometry and mechanics of tooth position in the white shark, *carcharodon carcharias*, *J. Morphol.* (1995) 277–288.
- [8] Bryan McNeil, Dayv Lowry, Shawn Larson, Denise Griffing, Feeding behavior of subadult sixgill sharks (*Hexanchus griseus*) at a bait station, *PLoS One* 11 (5) (2016).
- [9] Tim Tricas, J.E. McCosker, Predatory behavior of the white shark (*Carcharodon carcharias*), with notes on its biology, *Proc. – Calif. Acad. Sci.* 43 (1984) 221–238.
- [10] Philip J. Motta, Cheryl D. Wilga, Conservation and variation in the feeding mechanism of the spiny dogfish *squalus acanthias*, *J. Exp. Biol.* 201 (1998) 1345–1358.
- [11] Philip J. Motta, et al., Feeding mechanism and functional morphology of the jaws of the lemon shark *negaprion brevirostris* (chondrichthyes, carcharhinidae), *J. Exp. Biol.* 200 (1997) 2765–2780.
- [12] Philip J. Motta, Robert E. Hueter, Timothy C. Tricas, Adam P. Summers, J.D. McEachran, Kinematic analysis of suction feeding in the nurse shark, *Ginglymostoma cirratum* (Orectolobiformes, Ginglymostomatidae), *Copeia* 2002 (1) (2002) 24–38.
- [13] Abacus/CAE user's guide, Version 8.14-4, Chapter 13.4.1 Model instance data saved in input files, 2014.
- [14] Toni Laura Ferrara, Bite me: Mechanics of feeding in five species of sharks, PhD thesis The University of New South Wales, Australia (UNSW), 2012.
- [15] S. Wroel, D.R. Huber, M. Lowry, C. McHenry, K. Moreno, P. Clausen, T.L. Ferrara, E. Cunningham, M.N. Dean, A.P. Summers, Three-dimensional computer analysis of white shark jaw mechanics: how hard can a great white bite? *J. Zool.* 276 (2008) (2008) 336–342.